Report

Current Biology

Strigolactone- and Karrikin-Independent SMXL Proteins Are Central Regulators of Phloem Formation

Highlights

- *SMXL3/4/5* genes act as general promoters of phloem formation
- SMXL3/4/5 proteins are expressed and function very early during phloem development
- SMXL3/4/5 proteins do not mediate strigolactone or karrikin signaling
- Strigolactone/karrkin-dependent SMXL proteins are able to replace SMXL5

Authors

Eva-Sophie Wallner, Vadir López-Salmerón, Ilya Belevich, ..., Javier Agustí, Ivan Lebovka, Thomas Greb

Correspondence

thomas.greb@cos.uni-heidelberg.de

In Brief

Plants depend on long-distance transport of energy metabolites and signaling molecules along the phloem tissue. Wallner et al. show that phloem formation requires a family of proteins closely related to mediators of a hormonal signalling pathway. An hormone-independent action of the proteins analyzed is essential for robust phloem formation.

Wallner et al., 2017, Current Biology *27*, 1241–1247
April 24, 2017
http://dx.doi.org/10.1016/j.cub.2017.03.014

Current Biology
Report

Strigolactone- and Karrikin-Independent SMXL Proteins Are Central Regulators of Phloem Formation

Eva-Sophie Wallner,[1] Vadir López-Salmerón,[1] Ilya Belevich,[3] Gernot Poschet,[1] Ilona Jung,[1] Karin Grünwald,[2] Iris Sevilem,[3,4] Eija Jokitalo,[3] Rüdiger Hell,[1] Yrjö Helariutta,[3,4,5] Javier Agustí,[2,6] Ivan Lebovka,[1] and Thomas Greb[1,7,*]
[1]Centre for Organismal Studies (COS), Heidelberg University, Im Neuenheimer Feld 230, 69120 Heidelberg, Germany
[2]Gregor Mendel Institute (GMI), Austrian Academy of Sciences, Vienna Biocenter (VBC), Dr. Bohr-Gasse 3, 1030 Vienna, Austria
[3]Institute of Biotechnology, University of Helsinki, Viikinkaari 5d, 00014 Helsinki, Finland
[4]Department of Biological and Environmental Sciences, University of Helsinki, 00014 Helsinki, Finland
[5]Sainsbury Laboratory, University of Cambridge, Bateman Street, Cambridge CB2 1LR, UK
[6]Present address: Instituto de Biología Molecular y Celular de Plantas (IBMCP), Universidad Politecnica de Valencia, Ingeniero Fausto Elio, 46022 Valencia, Spain
[7]Lead Contact
*Correspondence: thomas.greb@cos.uni-heidelberg.de
http://dx.doi.org/10.1016/j.cub.2017.03.014

SUMMARY

Plant stem cell niches, the meristems, require long-distance transport of energy metabolites and signaling molecules along the phloem tissue. However, currently it is unclear how specification of phloem cells is controlled. Here we show that the genes *SUPPRESSOR OF MAX2 1-LIKE3* (*SMXL3*), *SMXL4*, and *SMXL5* act as cell-autonomous key regulators of phloem formation in *Arabidopsis thaliana*. The three genes form an uncharacterized subclade of the *SMXL* gene family that mediates hormonal strigolactone and karrikin signaling. Strigolactones are endogenous signaling molecules regulating shoot and root branching [1] whereas exogenous karrikin molecules induce germination after wildfires [2]. Both activities depend on the F-box protein and SCF (Skp, Cullin, F-box) complex component MORE AXILLARY GROWTH2 (MAX2) [3–5]. Strigolactone and karrikin perception leads to MAX2-dependent degradation of distinct SMXL protein family members, which is key for mediating hormonal effects [6–12]. However, the nature of events immediately downstream of SMXL protein degradation and whether all SMXL proteins mediate strigolactone or karrikin signaling is unknown. In this study we demonstrate that, within the *SMXL* gene family, specifically *SMXL3/4/5* deficiency results in strong defects in phloem formation, altered sugar accumulation, and seedling lethality. By comparing protein stabilities, we show that SMXL3/4/5 proteins function differently to canonical strigolactone and karrikin signaling mediators, although being functionally interchangeable with those under low strigolactone/karrikin signaling conditions. Our observations reveal a fundamental mechanism of phloem formation and indicate that diversity of SMXL protein functions is essential for a steady fuelling of plant meristems.

RESULTS

SMXL3, *SMXL4*, and *SMXL5* Act on Primary Root Growth

To reveal the function of the uncharacterized *SMXL* sub-clade 2 (Figure 1A), we phenotypically characterized single mutant seedlings as well as all possible double mutant combinations and the *smxl3;smxl4;smxl5* triple mutant (Figures S1A and S1B). In contrast to single mutants, which displayed no obvious phenotypic alterations to wild-type, primary root length was substantially reduced in all double mutants (Figures 1B and 1C), suggesting a redundant and equal contribution of all three genes to primary root growth. These defects were not observed in *smax1;smxl2* double or *smxl6;smxl7;smxl8* triple mutants, defective for *SMXL* sub-clades 1 and 3, respectively (Figure 1D). Strikingly, *smxl3;smxl4;smxl5* triple mutant seedlings were lethal (Figure 1E), while resembling double mutants at early growth stages (Figures 1B and 1F). This indicated a unique and dose-dependent role of the *SMXL3*, *SMXL4*, and *SMXL5* genes in growth regulation.

SMXL3, *SMXL4*, and *SMXL5* Are Expressed in Phloem-Associated Tissues

To see whether *SMXL3*, *SMXL4*, and *SMXL5* share similar expression patterns supporting functional redundancy, we stably expressed an endoplasmic reticulum (ER)-localized YELLOW FLUORESCENT PROTEIN (YFP) under the control of the respective promoters. As a reference we confirmed promoter activity of the karrikin (KAR) mediator *SMAX1* in the vasculature and columella (Figures S1C–S1E) [10, 13, 14]. *SMXL3* promoter activity was predominantly found in the root vasculature and weakly in the vasculature of cotyledons (Figures S1F–S1H). *SMXL4* and *SMXL5* promoter activities were specific for vascular tissues in all organs analyzed with a particular strong activity in root tips (Figures S1I–S1N), which was consistent with earlier findings for *SMXL4* [15, 16]. Close inspection of the root apical meristem

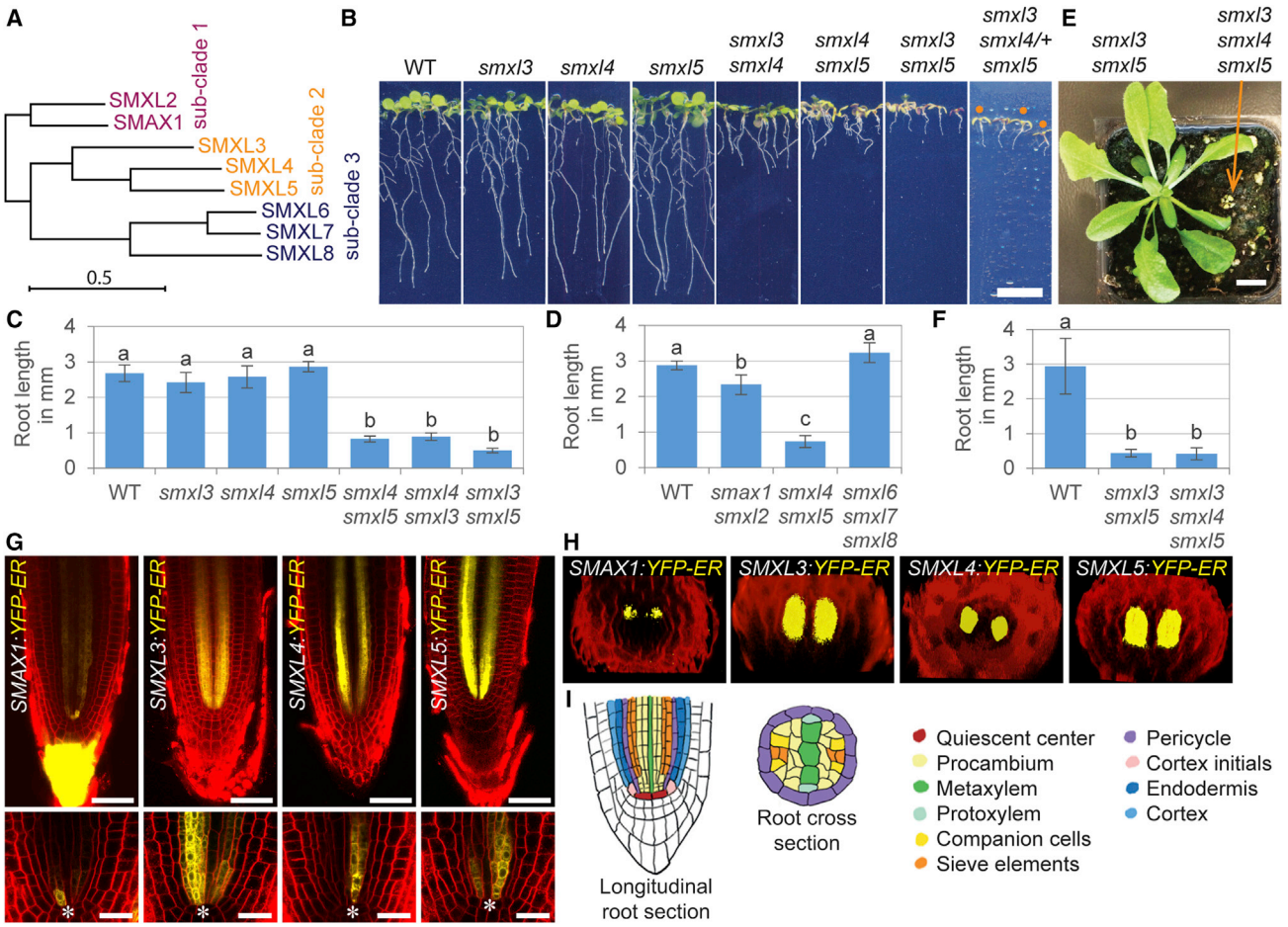

Figure 1. Phloem-Associated *SMXL3*, *SMXL4*, and *SMXL5* Genes Promote Root Growth

(A) A maximum likelihood phylogenetic tree based on amino acid sequence alignment of SMXL family members. The scale bar indicates a branch length with 0.5 amino acid substitutions per site.

(B) Root growth of 10-day-old seedlings. Homozygous *smxl3;smxl4;smxl5* seedlings are marked by orange dots. Scale bar represents 1 cm.

(C) Root length analysis from 3 independent experiments (n = 47–50 per experiment). Statistical groups indicated by letters were determined by one-way ANOVA with post hoc Tukey HSD (CI 95%).

(D) Root lengths analysis of 10-day-old seedlings from 4 independent experiments (n = 31–52 per experiment). Statistical groups determined by one-way ANOVA with post hoc Bonferroni test (CI 95%).

(E) Growth of *smxl3;smxl4;smxl5* mutants (indicated by an orange arrow). Scale bar represents 1 cm.

(F) Root length analysis of *smxl3;smxl4;smxl5* (n = 7) compared to wild-type and *smxl3;smxl5* (n = 48–61) plants. Statistical groups determined by one-way ANOVA with post hoc Tamhane-T2 (CI 95%).

(G) Root tips of 7-day-old seedlings. The overlay of YFP (yellow) and FM4-64 (red)-derived signals is depicted. Scale bars represent 50 μm (top) or 20 μm (bottom). The QC is marked by white asterisks.

(H) 3D reconstructed optical cross sections approximately 250 μm above the root tip.

(I) Schematic representations of RAM anatomy in a longitudinal section and a cross section of central tissues.

Error bars represent ± SD. See also Figure S1.

(RAM) revealed activities of all promoters immediately proximal to the quiescent center (QC) in sieve element (SE)-procambium stem cells and maturating phloem poles (Figure 1G). This finding was confirmed in cross sections that revealed *SMXL4* promoter activity in the two phloem poles and *SMXL3* and *SMXL5* promoter activities in both the developing phloem and the procambium (Figures 1H and 1I). In comparison, the *SMAX1* promoter was only weakly active in phloem-associated regions (Figures 1G–1I). Taking these observations together, we concluded that, in the RAM, *SMXL3*, *SMXL4*, and *SMXL5* promoters are specifically active in phloem-related tissues.

SMXL3, *SMXL4*, and *SMXL5* Promote Phloem Formation

To specify the function of *SMXL* sub-clade 2 members in root growth, we examined RAM anatomy of *smxl4;smxl5* mutants. Interestingly, the RAM size in *smxl4;smxl5* plants was indistinguishable from wild-type in 2-day-old seedlings, but decreased progressively over a period of 10 days (Figures 2A–2G). This suggested that maintaining RAM activity requires *SMXL4/5* gene functions.

Due to their phloem-associated expression and because phloem defects result in similar alterations in RAM performance [18, 19], we predicted a role of the *SMXL* sub-clade 2 in phloem

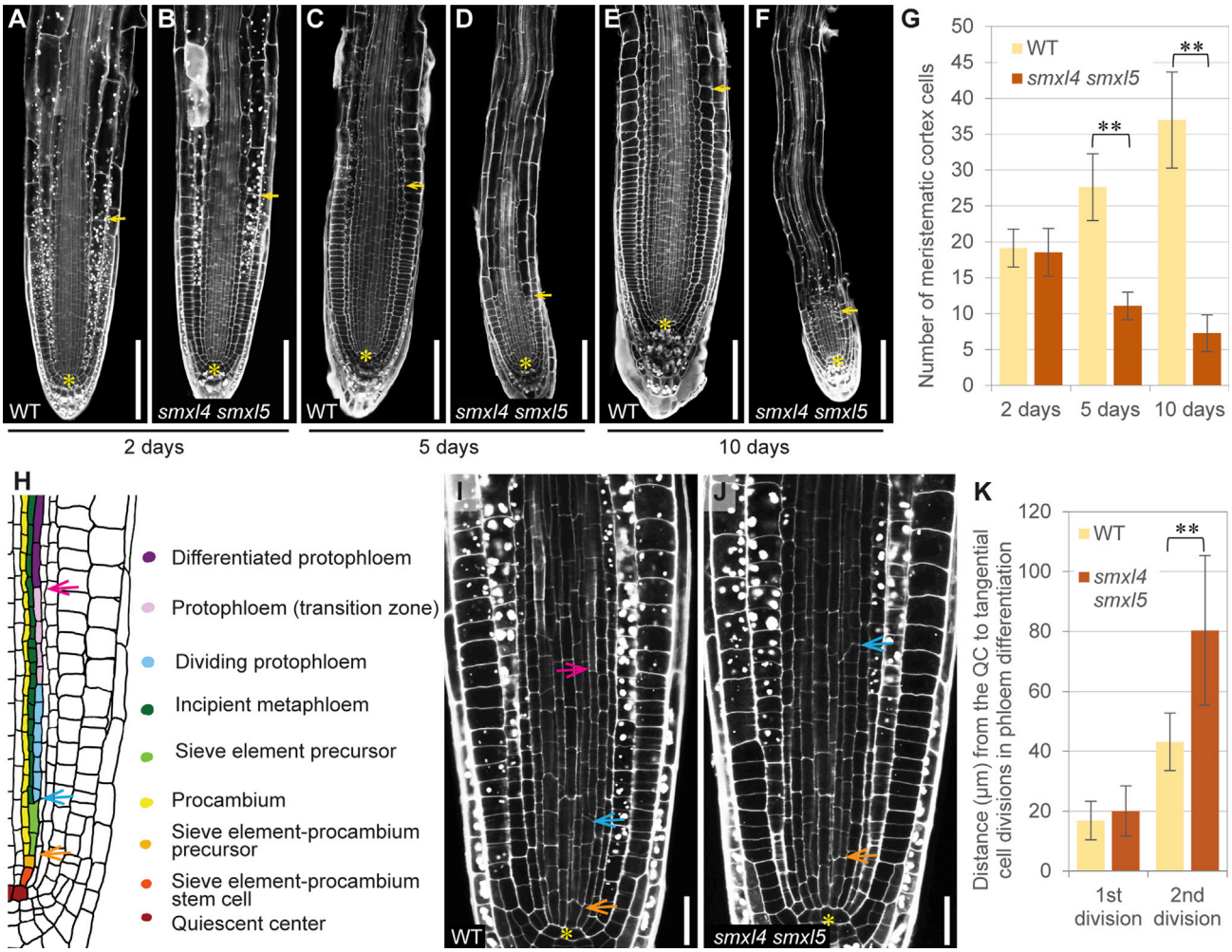

Figure 2. *smxl4;smxl5* Roots Lose RAM Activity over Time and Protophloem Differentiation Is Delayed

(A–F) Analyses of primary RAMs. Yellow arrows indicate the end of the meristematic zone [17]. Yellow asterisks mark the QC. Scale bars represent 100 µm.

(G) Quantification of the cortical cell number in the meristematic zone (n = 30–47). Welch's t test was performed comparing wild-type and *smxl4;smxl5* plants at each time point.

(H) Schematic overview of protophloem differentiation in roots. The first tangential cell division of the SE procambium-precursor is indicated by an orange arrow, the second tangential cell division of the SE precursor is marked by a blue arrow. The transition to differentiated protophloem SE strands is marked by a pink arrow.

(I and J) Tangential cell divisions in protophloem differentiation of 2-day-old roots. Arrows are described in (H). Differentiated sieve element are indicated by a pink arrow. Yellow asterisks indicate the QC. Scale bars represent 20 µm.

(K) Quantification of the distance of the first and second tangential cell division from the QC (n = 18). Welch's t test was performed.

Error bars represent ± SD.

formation. To test this, we investigated protophloem differentiation in 2-day-old seedlings when the *smxl4;smxl5* RAM size and the total number of stele cells was still unaffected (Figures 2G and S1O–S1Q). Indeed, *smxl4;smxl5* plants showed a delay in the second tangential cell division giving rise to proto- and metaphloem strands (Figures 2H–2K) [20]. Likewise, *smxl4;smxl5* RAMs were devoid of enhanced propidium iodide (PI) staining indicating differentiated SEs [21] (Figures 2I, 2J, S1O, and S1P). Reconstructions of 3D representations from ultrathin sections generated through serial block face scanning electron microscopy (SBEM) [22] confirmed that protophloem differentiation was substantially impaired in *smxl4;smxl5* plants. Cytosol density stayed high in cells located at positions expected for developing SEs (Figure 3A). In particular, enucleation, one of the first signs of SE differentiation in wild-type, was absent in *smxl4;smxl5* plants [24] (Figures 3B–3E). Moreover, activity of a *CALLOSE SYNTHASE7:H2B-YFP* (*CALS7:H2B-YFP*) marker visualizing nuclei of early protophloem cells prior to enucleation [24] was absent in *smxl4;smxl5* roots (Figures 3F and 3G). Taking these observations together, we concluded that early processes during SE formation are impaired in *smxl4;smxl5* RAMs.

To demonstrate a context-independent role of *SMXL4/5* in phloem formation, we investigated phloem differentiation capacity of *smxl5* and *smxl4;smxl5* cotyledons employing VISUAL [23, 25]. Before trans-differentiation, phloem appearance was comparable between wild-type and *smxl5* and *smxl4;smxl5*

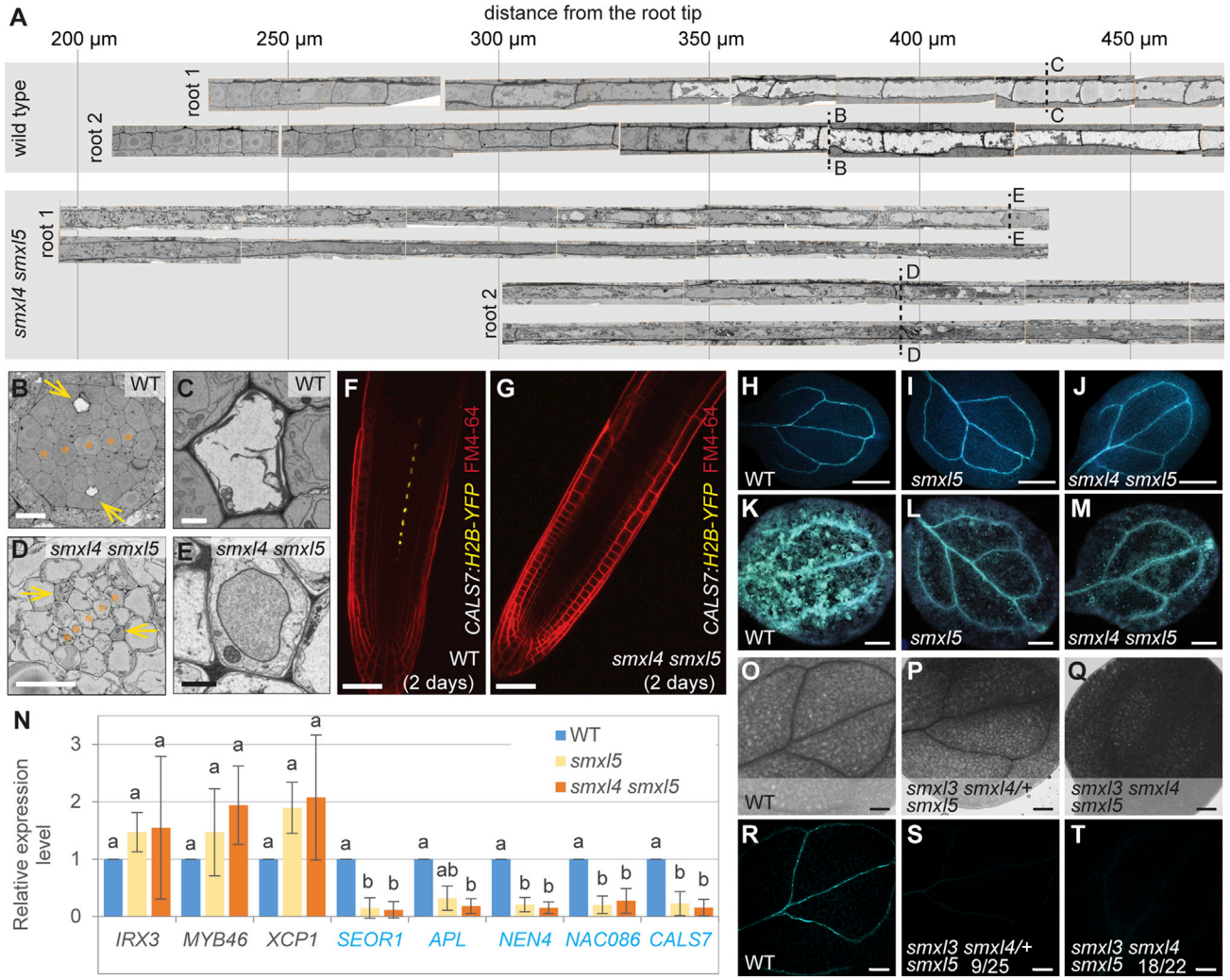

Figure 3. Phloem Formation Is Impaired in *smxl4;smxl5* and Absent in *smxl3;smxl4;smxl5* Mutants

(A–E) Characteristic longitudinal planes depicted from 3D volumetric SBEM datasets of differentiating protophloem strands from two individual roots. The dashed lines marked B–E indicate the locations of the cross-sections shown in (B)–(E). Developing protophloem strands are marked by yellow arrows and xylem poles by asterisks. Scale bars represent 10 µm in (B) and (D) and 1 µm in (C) and (E).

(F and G) Activity of the *CALS7:H2B-YFP* reporter. Scale bars represent 50 µm.

(H–J) Callose deposition in cotyledons visualized by aniline staining. Scale bars represent 100 µm.

(K–M) Aniline staining after VISUAL treatment [23] for 6 days. Scale bars represent 100 µm.

(N) After treatment (K–M), cotyledons of three independent experiments were used to determine transcript levels of genes. One-way ANOVA (CI 95%) with post hoc Bonferroni for datasets with homogeneous variances (*MYB46*, *XCP1*, *NEN4*, *NAC086*) or with post hoc Tamhane-T2 for datasets with inhomogeneous variances (*IRX3*, *SEOR1*, *APL*) was performed. Phloem-related genes are marked in blue, xylem-related genes in black.

(O–T) Cotyledons from 10-day-old plants shown under bright field (O–Q) or with aniline-based callose visualization (R–T). Scale bars represent 200 µm.

Error bars represent ± SD. See also Figures S2 and S3.

mutants (Figures 3H–3J). After inducing trans-differentiation, phloem abundance was lower in both *smxl5* and *smxl4;smxl5* mutants when compared to wild-type (Figures 3K–3M) and the increase of phloem-associated gene activity was less pronounced (Figure 3N). Supporting a specific role in phloem formation, no robust difference in xylem formation (Figures S2A–S2F) or in the induction of xylem-related genes was found.

Because we suspected that *SMXL3* activity masked a role of *SMXL4/5* in phloem strand formation under non-induced conditions, we analyzed the non-treated progeny of a viable *smxl3;smxl4/+;smxl5* plant. Indeed, 36% of *smxl3;smxl4/+;smxl5* plants and 82% of *smxl3;smxl4;smxl5* plants were devoid of phloem-related staining (Figures 3O–3T). Collectively, these findings indicated that *SMXL3/4/5* genes are early key regulators of phloem formation contributing in a dose-dependent manner.

Phloem Transport Capacities to the RAM Are Reduced in *smxl4;smxl5* Plants

To assess the impact of the observed defects on phloem-based transport to the RAM, we investigated phloem-dependent movement in wild-type and *smxl4;smxl5* roots. Grafting of wild-type

shoots onto *smxl4;smxl5* mutant roots did not improve root growth (Figures S2G and S2H). Interestingly, leaves of all grafts supported by *smxl4;smxl5* roots were smaller and accumulated more sucrose while all leaves supported by wild-type roots had no defect (Figures S2I and S2J). Likewise, sugar exudation from *smxl5* and *smxl4;smxl5* leaves was not impaired but was according to the overall sugar levels found in our direct measurements (Figures S2J and S2K). Together, these observations showed that phenotypic alterations in shoots were a secondary effect of *SMXL4/5* deficiency in roots.

Indeed, when wild-type shoots containing the *SUCROSE TRANSPORTER 2:GREEN FLUORESCENT PROTEIN* (*SUC2:GFP*) transgene [26] were grafted onto wild-type or *smxl4;smxl5* roots, weaker GFP intensities were observed in tips of the longest *smxl4;smxl5* root compared to wild-type root tips (Figures S2L and S2M). Of note, at the stage of analysis, the primary root of *smxl4;smxl5* plants was shorter than the lateral roots and did not display any GFP fluorescence at the tip (Figures S2N and S2O). These findings indicated reduced phloem-dependent transport to the *smxl4;smxl5* RAM.

SMXL4 and *SMXL5* Do Not Mediate SL/KAR Signaling

To see whether *SMXL4/5*, like other SMXL family members [8, 10, 13, 14], act as strigolactone (SL) or KAR signaling mediators, we analyzed root growth and protophloem formation in *max2* single and *smxl4;smxl5;max2* triple mutants. Interestingly, *smxl4;smxl5;max2* mutants were indistinguishable from *smxl4;smxl5* mutants in terms of root length and RAM size (Figures S3A–S3G). In particular, tangential cell divisions of SE precursor cells were as delayed in *smxl4;smxl5;max2* triple as in *smxl4;smxl5* double mutants (Figures S3H–S3L). Furthermore, *max2* mutants initiated those divisions just like wild-type plants (Figures S3I and S3J). Likewise, formation of protophloem-derived SEs was similarly impaired in both *smxl4;smxl5* and *smxl4;smxl5;max2* plants (Figures S3M–S3P). Those findings argued for a *MAX2*-independent role of *SMXL4* and *SMXL5* in promoting phloem differentiation and RAM activity and against a role as mediators of *MAX2*-dependent SL/KAR signaling.

SMAX1 Can Functionally Replace SMXL5, but Only SMAX1 Stability Is SL/KAR Dependent

To see whether the lack of genetic interaction between *SMXL4/5* and the SL/KAR signaling pathway is reflected by differences in SL/KAR-dependent protein degradation, we compared stabilities of SMXL3-YFP, SMXL4-YFP, SMXL5-YFP, and SMAX1-YFP fusion proteins expressed stably in plants. To exclude that different sites of protein accumulation affect SL/KAR responsiveness, we first expressed SMXL5-YFP and SMAX1-YFP fusion proteins under the control of the *SMXL5* promoter in *smxl4;smxl5* mutants. As a result, not only the *SMXL5:SMXL5-YFP* but also the *SMXL5:SMAX1-YFP* transgene suppressed the growth defect usually observed in *smxl4;smxl5* roots (Figures 4A and 4B). This demonstrated that both proteins were active and, importantly, that SMAX1 was able to replace SMXL5 when present in the same cells. Interestingly, when grown with *rac*-GR24 triggering both SL and KAR signaling [12], the compensatory effect of the *SMXL5:SMAX1-YFP* transgene on *smxl4;smxl5* root length was lost, while the *SMXL5:SMXL5-YFP* transgene was still able to fully restore growth of *smxl4;smxl5* roots (Figures 4A and 4B).

To determine whether the *rac*-GR24-dependent difference between SMAX1-YFP and SMXL5-YFP was reflected by different protein stabilities, we investigated YFP intensities in root tips after short-term *rac*-GR24 treatments. Overlapping with sites of *SMXL5* promoter activity (Figure 1), SMXL5-YFP and SMAX1-YFP proteins were localized to the nuclei of developing phloem cells and SMAX1-YFP and SMXL5-YFP levels were comparable when incubated without *rac*-GR24 (Figures 4C and 4E). As expected, the SMAX1-YFP signal started fading around 8 min after the onset of *rac*-GR24 treatments and was completely gone after 12 min (Figure 4D). In contrast, the SMXL5-YFP signal remained unaffected, even when treatment was maintained for 1 hr (Figures 4F and 4G). Similar to SMXL5-YFP, levels of SMXL3-YFP and SMXL4-YFP were unaffected by *rac*-GR24 when expressed under the control of their own promoters (Figure S4). Thus, stabilities of SMAX1 but not of SMXL subclade 2 members are *rac*-GR24 dependent.

DISCUSSION

In this study, we provide evidence that the *Arabidopsis SMXL3*, *SMXL4*, and *SMXL5* genes promote phloem development. In addition, we provide evidence that SMXL3, SMXL4, and SMXL5 activities do not depend on SL/KAR signaling components acting on other SMXL family members. Collectively, we demonstrate a role of SMXL3/4/5 proteins as SL/KAR-independent developmental triggers of long-distance transport capacities.

Several functionally tightly interconnected genes have been identified to act in protophloem differentiation in the RAM [27]. Interestingly, none of the described phloem-defective mutants shows all the defects observed in *smxl4;smxl5* plants. For example, similar to *smxl4;smxl5*, *brevis radix* (*brx*) mutants show a delay or absence of the second tangential cell division of the SE precursor cell linage [28]. Similar defects are found in *OCTOPUS* (*OPS*)-deficient plants [29]. In both *ops* and *brx* mutants, protophloem differentiation is affected, which is reflected by the presence of undifferentiated "gap" cells alternating with differentiated SEs [18, 19]. This phenotype is common among several protophloem-defective mutants for which *cotyledon vascular pattern2* (*cvp2*);*cvp2-like 1* (*cvl1*) double mutants are another example [19]. Along the same lines, ALTERED PHLOEM DEVELOPMENT (APL)-defective mutants show defects in phloem differentiation but normal protophloem development including cell wall thickening, which is absent in *smxl4;smxl5* [21, 30]. In contrast, *smxl4;smxl5* plants display a general block of SE formation, suggesting that the *SMXL4/5* gene functions are more central.

Interestingly, over-accumulation of CLAVATA3/ENDOSPERM SURROUNDING REGION 45 (CLE45) peptides triggers a similar block of SE differentiation as observed in *smxl4;smxl5* mutants [18]. The putative receptor of CLE45 is the leucine-rich repeat receptor-like kinase BARELY ANY MERISTEM 3 (BAM3) [18]. However, we found the *SMXL3/4/5* promoters to be active already in SE-procambium stem cells whereas *CLE45* and *BAM3* expression appears first in SE precursor cells [27]. This may argue for an earlier role of *SMXL3/4/5* in phloem formation.

Our genetic analyses and analyses of SMXL3/4/5 protein stability suggest that the activities of SMXL4 and SMXL5 proteins do not depend on known components of the SL/KAR signaling

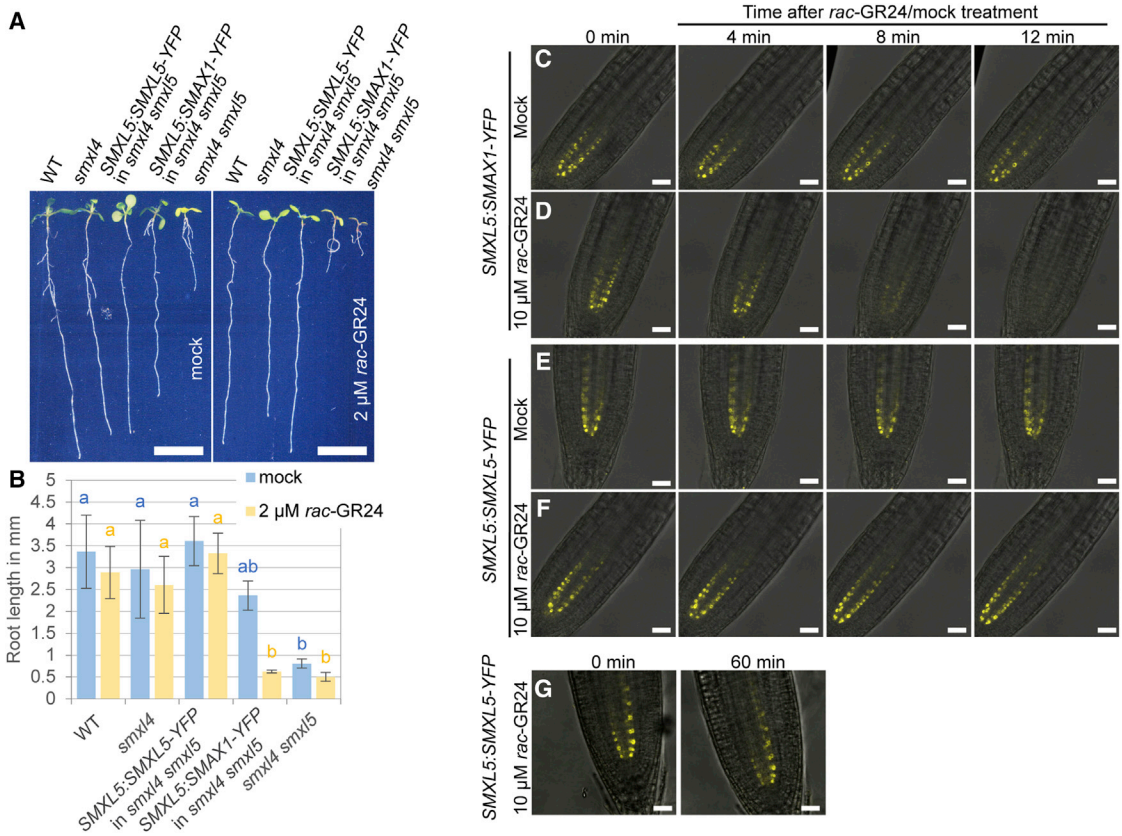

Figure 4. *SMXL5* Can Be Replaced by *SMAX1* but Does Not Depend on SL/KAR Signaling

(A and B) Root lengths of 10-day-old seedlings. Scale bars represent 1 cm (3 independent experiments, n = 27–55 each). Statistical groups were determined by one-way ANOVA with post hoc Bonferroni (CI 95%) separately for the datasets "mock" and "*rac*-GR24."

(C–G) 5-day-old *smxl4;smxl5* root tips. Shown are overlaps of bright field (gray) and YFP-derived signals (yellow). Scale bars represent 25 μm.

Error bars represent ± SD. See also Figure S4.

machinery. The observation that the sequence motif identified to be important for MAX2/D14-dependent ubiquitination [6, 7] is not conserved in members of sub-clade 2 [14, 31] is in line with this idea. In fact, reduction of SMXL4/5 activity did not result in the suppression of enhanced branching observed in *max2* mutants, again arguing for an SL-independent role [14]. Moreover, *smxl4;smxl5;max2* mutants were indistinguishable from *smxl4;smxl5* mutants, which argues against a *MAX2*-dependent contribution of other SMXL proteins to phloem development. However, this interpretation is based on the assumption that other SMXL proteins are under the control of SL/KAR signaling in early root development and, more specifically, in developing phloem cells. Because SL/KAR signaling naturally depends on endogenous SL/KAR levels which could be low in those cells at this stage, we cannot exclude that SL/KAR signaling regulates phloem formation at other times or places. In fact, phloem tissues proved to be perceptive to SL/KAR signaling but SMAX1-YFP levels were as high as SMXL5-YFP levels without *rac*-GR24 treatments.

In summary, beyond being essential mediators of SL/KAR signaling and plant growth plasticity [32], SMXL proteins are central regulators of phloem formation and general plant growth. The three SMXL sub-clades not only hold different regulatory roles, but also have fundamental differences in protein function. Independence of SMXL3, SMXL4, and SMXL5 from SL/KAR signaling may be crucial for a robust formation of long-distance transport capacities and, consequently, plant vitality.

SUPPLEMENTAL INFORMATION

Supplemental Information includes four figures and Supplemental Experimental Procedures and can be found with this article online at http://dx.doi.org/10.1016/j.cub.2017.03.014.

AUTHOR CONTRIBUTIONS

E.-S.W. and T.G. conceived and designed the experiments. E.-S.W., V.L.-S., I.J., K.G., I.S., G.P., I.L., Y.H., J.A., I.B., E.J., and R.H. performed the experiments. E.-S.W., G.P., T.G., I.B., and V.L.-S. analyzed the data. E.-S.W. and T.G. wrote the paper.

ACKNOWLEDGMENTS

This work was supported by DFG grant GR 2104/4-1, a Heisenberg Professorship (DFG, GR 2104/5-1), and an ERC Consolidator grant (PLANTSTEMS, #647148) to T.G. This work was also supported by the COST Action STREAM (FA1206). We would like to thank the Metabolomics Core Technology Platform of the Excellence Initiative Heidelberg supported by grant ZUK 49/2 (DFG) for ion chromatography-based metabolite quantification. E.J., I.B., and SB-EM imaging are supported by Biocenter Finland. Mervi Lindman and Antti Salminen (University of Helsinki, Finland) are acknowledged for technical assistance

in sample preparation for SB-EM. Y.H. laboratory was funded by the Gatsby Foundation (GAT3395/PR3), the NSF BBSRC grant BB/N013158/1, University of Helsinki (award 799992091), the ERC Advanced Investigator Grant SYMDEV, Tekes (the Finnish Funding Agency for Technology and Innovation), and the Academy of Finland Centre of Excellence programme (award 63053034). Charles Melnyk (Sainsbury Laboratory, University of Cambridge, UK) helped with the grafting technique. David Nelson (University of California Riverside, USA) provided *smax1-2*, *smax1-2;smxl2-1*, and *smxl6-4;smxl7-3;smxl8-1* mutant seeds.

Received: January 10, 2017
Revised: March 1, 2017
Accepted: March 8, 2017
Published: April 6, 2017

REFERENCES

1. Borghi, L., Liu, G.W., Emonet, A., Kretzschmar, T., and Martinoia, E. (2016). The importance of strigolactone transport regulation for symbiotic signaling and shoot branching. Planta *243*, 1351–1360.
2. Waters, M.T., Scaffidi, A., Sun, Y.K., Flematti, G.R., and Smith, S.M. (2014). The karrikin response system of *Arabidopsis*. Plant J. *79*, 623–631.
3. Nelson, D.C., Scaffidi, A., Dun, E.A., Waters, M.T., Flematti, G.R., Dixon, K.W., Beveridge, C.A., Ghisalberti, E.L., and Smith, S.M. (2011). F-box protein MAX2 has dual roles in karrikin and strigolactone signaling in *Arabidopsis thaliana*. Proc. Natl. Acad. Sci. USA *108*, 8897–8902.
4. Waters, M.T., and Smith, S.M. (2013). KAI2- and MAX2-mediated responses to karrikins and strigolactones are largely independent of HY5 in *Arabidopsis* seedlings. Mol. Plant *6*, 63–75.
5. Stirnberg, P., Furner, I.J., and Ottoline Leyser, H.M. (2007). MAX2 participates in an SCF complex which acts locally at the node to suppress shoot branching. Plant J. *50*, 80–94.
6. Jiang, L., Liu, X., Xiong, G., Liu, H., Chen, F., Wang, L., Meng, X., Liu, G., Yu, H., Yuan, Y., et al. (2013). DWARF 53 acts as a repressor of strigolactone signalling in rice. Nature *504*, 401–405.
7. Zhou, F., Lin, Q., Zhu, L., Ren, Y., Zhou, K., Shabek, N., Wu, F., Mao, H., Dong, W., Gan, L., et al. (2013). D14-SCF(D3)-dependent degradation of D53 regulates strigolactone signalling. Nature *504*, 406–410.
8. Wang, L., Wang, B., Jiang, L., Liu, X., Li, X., Lu, Z., Meng, X., Wang, Y., Smith, S.M., and Li, J. (2015). Strigolactone signaling in *Arabidopsis* regulates shoot development by targeting D53-Like SMXL repressor proteins for ubiquitination and degradation. Plant Cell *27*, 3128–3142.
9. Conn, C.E., Bythell-Douglas, R., Neumann, D., Yoshida, S., Whittington, B., Westwood, J.H., Shirasu, K., Bond, C.S., Dyer, K.A., and Nelson, D.C. (2015). PLANT EVOLUTION. Convergent evolution of strigolactone perception enabled host detection in parasitic plants. Science *349*, 540–543.
10. Stanga, J.P., Morffy, N., and Nelson, D.C. (2016). Functional redundancy in the control of seedling growth by the karrikin signaling pathway. Planta *243*, 1397–1406.
11. Liang, Y., Ward, S., Li, P., Bennett, T., and Leyser, O. (2016). SMAX1-LIKE7 signals from the nucleus to regulate shoot development in *Arabidopsis* via partially EAR motif-independent mechanisms. Plant Cell *28*, 1581–1601.
12. Li, S., Chen, L., Li, Y., Yao, R., Wang, F., Yang, M., Gu, M., Nan, F., Xie, D., and Yan, J. (2016). Effect of GR24 stereoisomers on plant development in *Arabidopsis*. Mol. Plant *9*, 1432–1435.
13. Stanga, J.P., Smith, S.M., Briggs, W.R., and Nelson, D.C. (2013). SUPPRESSOR OF MORE AXILLARY GROWTH2 1 controls seed germination and seedling development in *Arabidopsis*. Plant Physiol. *163*, 318–330.
14. Soundappan, I., Bennett, T., Morffy, N., Liang, Y., Stanga, J.P., Abbas, A., Leyser, O., and Nelson, D.C. (2015). SMAX1-LIKE/D53 family members enable distinct MAX2-dependent responses to strigolactones and karrikins in *Arabidopsis*. Plant Cell *27*, 3143–3159.
15. Zhang, L., Yang, T., Li, X., Hao, H., Xu, S., Cheng, W., Sun, Y., and Wang, C. (2014). Cloning and characterization of a novel Athspr promoter specifically active in vascular tissue. Plant Physiol. Biochem. *78*, 88–96.
16. Yang, T., Zhang, L., Hao, H., Zhang, P., Zhu, H., Cheng, W., Wang, Y., Wang, X., and Wang, C. (2015). Nuclear-localized AtHSPR links abscisic acid-dependent salt tolerance and antioxidant defense in *Arabidopsis*. Plant J. *84*, 1274–1294.
17. Beemster, G.T., and Baskin, T.I. (1998). Analysis of cell division and elongation underlying the developmental acceleration of root growth in *Arabidopsis thaliana*. Plant Physiol. *116*, 1515–1526.
18. Depuydt, S., Rodriguez-Villalon, A., Santuari, L., Wyser-Rmili, C., Ragni, L., and Hardtke, C.S. (2013). Suppression of *Arabidopsis* protophloem differentiation and root meristem growth by CLE45 requires the receptor-like kinase BAM3. Proc. Natl. Acad. Sci. USA *110*, 7074–7079.
19. Rodriguez-Villalon, A., Gujas, B., van Wijk, R., Munnik, T., and Hardtke, C.S. (2015). Primary root protophloem differentiation requires balanced phosphatidylinositol-4,5-biphosphate levels and systemically affects root branching. Development *142*, 1437–1446.
20. Rodriguez-Villalon, A. (2016). Wiring a plant: genetic networks for phloem formation in *Arabidopsis thaliana* roots. New Phytol. *210*, 45–50.
21. Truernit, E., Bauby, H., Dubreucq, B., Grandjean, O., Runions, J., Barthélémy, J., and Palauqui, J.C. (2008). High-resolution whole-mount imaging of three-dimensional tissue organization and gene expression enables the study of phloem development and structure in *Arabidopsis*. Plant Cell *20*, 1494–1503.
22. Denk, W., and Horstmann, H. (2004). Serial block-face scanning electron microscopy to reconstruct three-dimensional tissue nanostructure. PLoS Biol. *2*, e329.
23. Kondo, Y., Nurani, A.M., Saito, C., Ichihashi, Y., Saito, M., Yamazaki, K., Mitsuda, N., Ohme-Takagi, M., and Fukuda, H. (2016). Vascular cell induction culture system using *Arabidopsis* leaves (VISUAL) reveals the sequential differentiation of sieve element-like cells. Plant Cell *28*, 1250–1262.
24. Furuta, K.M., Yadav, S.R., Lehesranta, S., Belevich, I., Miyashima, S., Heo, J.O., Vatén, A., Lindgren, O., De Rybel, B., Van Isterdael, G., et al. (2014). Plant development. *Arabidopsis* NAC45/86 direct sieve element morphogenesis culminating in enucleation. Science *345*, 933–937.
25. Kondo, Y., Fujita, T., Sugiyama, M., and Fukuda, H. (2015). A novel system for xylem cell differentiation in Arabidopsis thaliana. Mol. Plant *8*, 612–621.
26. Vatén, A., Dettmer, J., Wu, S., Stierhof, Y.D., Miyashima, S., Yadav, S.R., Roberts, C.J., Campilho, A., Bulone, V., Lichtenberger, R., et al. (2011). Callose biosynthesis regulates symplastic trafficking during root development. Dev. Cell *21*, 1144–1155.
27. Rodriguez-Villalon, A., Gujas, B., Kang, Y.H., Breda, A.S., Cattaneo, P., Depuydt, S., and Hardtke, C.S. (2014). Molecular genetic framework for protophloem formation. Proc. Natl. Acad. Sci. USA *111*, 11551–11556.
28. Scacchi, E., Salinas, P., Gujas, B., Santuari, L., Krogan, N., Ragni, L., Berleth, T., and Hardtke, C.S. (2010). Spatio-temporal sequence of cross-regulatory events in root meristem growth. Proc. Natl. Acad. Sci. USA *107*, 22734–22739.
29. Truernit, E., Bauby, H., Belcram, K., Barthélémy, J., and Palauqui, J.C. (2012). OCTOPUS, a polarly localised membrane-associated protein, regulates phloem differentiation entry in *Arabidopsis thaliana*. Development *139*, 1306–1315.
30. Bonke, M., Thitamadee, S., Mähönen, A.P., Hauser, M.T., and Helariutta, Y. (2003). APL regulates vascular tissue identity in *Arabidopsis*. Nature *426*, 181–186.
31. Wallner, E.S., López-Salmerón, V., and Greb, T. (2016). Strigolactone versus gibberellin signaling: reemerging concepts? Planta *243*, 1339–1350.
32. Domagalska, M.A., and Leyser, O. (2011). Signal integration in the control of shoot branching. Nat. Rev. Mol. Cell Biol. *12*, 211–221.